

## Characterization of the ZnSe/ZnS Core Shell Quantum Dots Synthesized at Various Temperature Conditions and the Water Soluble ZnSe/ZnS Quantum Dot

Cheong-Soo Hwang\* and Ill-Hee Cho

Department of Chemistry, Institute of Nanosensor and Biotechnology, Dankook University, Seoul 140-714, Korea

\*E-mail: cshwang@dankook.ac.kr

Received July 20, 2005

ZnSe/ZnS, UV-blue luminescent core shell quantum dots, were synthesized *via* a thermal decomposition reaction of organometallic zinc and solvent coordinated Selenium (TOPSe) in a hot solvent mixture. The synthetic conditions of the core (ZnSe) and the shell (ZnS) were independently studied at various reaction temperature conditions. The obtained colloidal nanocrystals at corresponding temperatures were characterized for their optical properties by UV-vis, room temperature solution photoluminescence (PL) spectroscopy, and further obtained powders were characterized by XRD, TEM, and EDXS analyses. The synthetic temperature condition to obtain the best PL emission intensity for the ZnSe core was 300 °C, and for the optimum shell capping, the temperature was 135 °C. At this temperature, solution PL spectrum showed a narrow emission peak at 427 nm with a PL efficiency of 15%. In addition, the measured particle sizes for the ZnSe/ZnS nanocomposite *via* TEM were in the range of 5 to 12 nm. Furthermore, we have synthesized water-soluble ZnSe/ZnS nanoparticles by capping the ZnSe/ZnS hydrophobic surface with mercaptoacetate (MAA) molecules. For the obtained aqueous colloidal solution, the UV-vis spectrum showed an absorption peak at 250 nm, and the solution PL emission spectrum showed a peak at 425 nm, which is similar to that for hydrophobic quantum dot ZnSe/ZnS. However, the calculated PL efficiency was relatively low (0.1%) due to the luminescence quenching by water and MAA molecules. The capping ligand was also characterized by FT-IR spectroscopy, with the carbonyl stretching peak in the mercaptoacetate molecule appearing at 1575 cm<sup>-1</sup>. Finally, the particle sizes of the MAA capped ZnSe/ZnS were measured by TEM, showing a range of 12 to 17 nm.

**Key Words :** ZnSe/ZnS quantum dot, Water soluble quantum dot, UV-blue emission, Semiconductor nanocrystal, Photoluminescence

### Introduction

Semiconductor nanocrystals, or quantum dots, have gained considerable interest during the past decade.<sup>1,2</sup> These materials offer unique technological applications for various photoelectronic devices or even for advanced biotechnology due to their size dependant physical and optical properties.<sup>3-5</sup> Recently developed nanocrystallite ZnSe is of special interest due to their intense UV blue luminescent properties, an emission wavelength at 460 nm and a band gap of 2.7 eV, properties not observed in other nanocomposite materials, such as CdS, ZnS, and CdSe.<sup>6-8</sup> In addition, it has been reported that when the surface of ZnSe is passivated by ZnS, a ZnSe/ZnS core shell quantum dot is formed and the quantum yield is greatly improved compared with that for the bare ZnSe.<sup>9</sup> In that paper, and as we followed the same procedures, the ZnSe/ZnS nanocrystal was prepared from the reaction of diethyl zinc with solvent coordinated selenium in a hot solvent, giving the core ZnSe, and then the reaction of diethyl zinc with hexamethyldisilathiane for the shell ZnS layer. The measured ZnSe/ZnS particle sizes *via* a HR-TEM image were in the range of 3.5–4.6 nm, and the luminescence quantum yield for the ZnSe/ZnS nanocrystal was up to 20 times more than that for the bare ZnSe. However, to our knowledge, the reaction conditions at

various temperatures for core ZnSe and the shell capping together has not intensively investigated.

Water soluble quantum dot materials were developed for the biosensing materials, bonding to biomolecules, such as DNAs or proteins.<sup>10-12</sup> Those materials are expected to replace complicated or health-hazardous radioactive detections and become the basis of very sensitive biological assays. Semiconductor nanocrystals are also proven to be much more efficient, sensitive, and stable than the organic dyes used for the same purpose. The most common assay method is to prepare water soluble quantum dots by capping their surface with polar solvent molecules such as mercaptoacetic acid, aminoacid or dihydrolipoic acid; then the target biomolecules are attached *via* covalent bonding or self assembly. In this area CdSe/ZnS or CdS/ZnS quantum dots are most commonly used since their emission wavelengths are in the visible light region.<sup>2,6</sup> The CdS core and ZnS shell have a lattice mismatch of 7%, and their band gaps are 2.58 and 3.83 eV, respectively.<sup>13</sup> In contrast, ZnSe/ZnS quantum dots are rarely applied in biological detection, probably due to their wide band gap, which results in a UV-blue luminescence property. However, recently Eychmuller *et al.* reported synthesis of a water-soluble ZnSe.<sup>14</sup> The hydrophobic semiconductor was passivated with thiol stabilizers and further photochemical treatment caused great

enhancement of PL intensity. The water soluble nanocrystal was used for the fabrication of UV-blue emitting film, which can be applied in various areas, including biotechnology.

In this paper we describe the synthesis and characterization of the size and optical properties of the ZnSe/ZnS quantum dots prepared at various reaction conditions. In addition, we report the synthesis and optical properties of new water soluble ZnSe/ZnS semiconductor nanocrystal.

## Experimental Section

**General Procedures.** All the solvents used (*n*-hexane, methanol, chloroform and butanol) were purchased from Aldrich and distilled before use. Diethylzinc (0.1 M solution in hexane), hexadecylamine (HDA, 90%), tri-*n*-octylphosphine (TOP, 90%), and Selenium powder (~100 mesh 99.999%) were purchased from Aldrich and used as received. Hexamethyldisilathiane, (TMS)<sub>2</sub>S, was purchased from Fluka and used without further purification. 1 M (TOP)Se stock solution was prepared in a dry box *via* mixing of 0.78 g (0.01 mol) of Se powder with TOP solvent so that the total volume of the solution reached 10 mL in a volumetric flask. The UV-vis spectrum was recorded on a SCINCO 2001 spectrophotometer equipped with a deuterium/tungsten lamp. The solution IR spectrum was recorded on a Bruker IRS-66/S spectrophotometer. The PL spectrum was taken in a DARSA-2000 spectrophotometer equipped with a 500 W Xenon lamp, 0.275 m triple grating monochromator, and PHV 400 photomultiplitor tube. The PL efficiencies for the corresponding bare ZnSe, ZnSe/ZnS quantum dot, and water soluble ZnSe/ZnS quantum dot materials were calculated by comparing to the recommended standard material in literature,<sup>15</sup> 0.1 M solution of Quinine sulfate in H<sub>2</sub>SO<sub>4</sub> (Fluka) whose excitation wave length and reported absolute quantum yield are 350 nm and 0.546 at room temperature. The powder XRD pattern diagram was obtained by using Rigaku 300 X-ray diffractometer with Cu K $\alpha$  (1.54 Å) wavelength light source. TEM images were taken with a JEOL JEM 1210 electron microscope with a MAG mode of 1000 to 800000, and the accelerating voltage was 40–120 kV. The samples for the TEM were prepared *via* dispersion into hexane solvent and placement on a carbon-coated copper grid (300 Mesh) followed by drying under vacuum. In addition, the elemental composition of the quantum dot was determined by an EDXS (Energy Dispersive X-ray Spectroscopy) spectrum which was obtained *via* an EDXS collecting unit equipped in the TEM, with a Si (Li) detector in IXRF 500 system.

**Synthesis of the Core ZnSe at Various Temperatures.** The preparation method was slightly modified from the previously method reported in the literature.<sup>9</sup> All the manipulations were carried out using modified Schlenk techniques under an inert atmosphere of Argon. 15 mL of HDA solvent were placed in a 200 mL three-neck flask connected to a vacuum manifold. The liquid was dried and degassed under vacuum at *ca.* 125 °C for 7 hours, and then the flask was filled with argon gas. Prepared 1 M TOPSe

stock solution 0.6 mL was taken out with a glass syringe from the dry box, and immediately transferred to the flask containing the hot HDA solvent. Further addition of 6 mL of 0.1 M Et<sub>2</sub>Zn (0.6 mmol) solution was carried out under various temperature conditions from 250 to 320 °C. After mixing the two precursors, a vigorous reaction occurred immediately, and the mixture was stirred for 30 minutes at each corresponding temperature. 0.1 mL of hot aliquots were carefully taken from each sample *via* glass syringe and were suspended immediately into 30 mL hexane containing vials to measure solution PL spectra.

**Capping of the Core ZnSe with ZnS at Various Temperatures.** The ZnSe/ZnS quantum dot was simply prepared by the addition of zinc and sulfur precursors to the ZnSe core so that the shell ZnS layer formed on the surface of the ZnSe core. For these experiments, the preparation condition for the bare ZnSe was fixed at 300 °C since we have obtained the best PL intensity at this temperature. After addition of the two Zn and Se precursors at 300 °C, the flask was cooled for further addition of zinc and sulfur precursors. A mixture of 7 mL of 0.1 M Et<sub>2</sub>Zn (0.7 mmol) and 0.13 mL of (TMS)<sub>2</sub>S (0.6 mmol) in TOP solvent was added drop wise at the reaction temperatures of 125, 135, 155, 175, and 195 °C. After 30 minutes of stirring at the corresponding temperature, 0.1 mL of hot aliquots were carefully taken from each sample *via* glass syringe and were suspended immediately into 30 mL hexane containing vials to measure solution PL spectra.

**Synthesis of the Water Soluble ZnSe/ZnS Quantum Dot.** At first the hydrophobic ZnSe/ZnS quantum dot powder was prepared by exactly following the previously reported method, including size selective precipitation *via* multiple centrifuging and filtering steps.<sup>9</sup> Synthesized ZnSe/ZnS quantum dot white powder was redispersed in 25 mL chloroform solvent. A 50 mL sample of 0.1 M solution of mercaptoacetic acid (MAA) in methanol was placed in a separate flask. 1 M stock solution of KOH was added until the PH reached 10. A 15 mL sample of the MAA-KOH mixed solution was transferred to the flask containing ZnSe/ZnS nanocrystal. After stirring 3 hours, phosphate buffer saline (PBS) solution was added. The upper layer was isolated by separate funnel, and the excess MAA was removed by centrifuging. The colloidal aqueous solution was characterized by UV-vis, liquid IR, and liquid PL spectroscopy. Trials to obtain powder out of this aqueous solution under vacuum were not successful; however, we were able to obtain TEM images by placing a drop of the aqueous solution on the copper grids and drying in a vacuum oven overnight.

## Results and Discussions

The most common synthetic scheme for the ZnSe nanocrystal is to use pyrophoric organometallic precursors of diethylzinc<sup>6</sup> or organoselenium<sup>16,17</sup> compounds in coordinating hot solvents. Optical properties of the ZnSe nanocrystals have been shown by Reiss *et al.* to be strongly

depend on the mixing temperature of the zinc and selenium precursors in the coordinating solvent.<sup>18</sup> In that paper the authors observed that the prepared ZnSe at 250 °C showed small and broad UV-vis absorption peak at 395 nm, whereas the same compound made at 300 °C showed a red shift toward to 426 nm. The sizes of the particles prepared at those two temperatures are approximately the same, averaging 3 nm for 250 °C and average 4.7 nm for 300 °C according to TEM analyses. In addition, the PL spectrum showed a narrow and sharp peaks from 390 (for 250 °C) to 440 nm (for 300 °C) wavelengths region.

In our study we fixed the molar ratio between Zn and S at 1 : 1, and then we varied the mixing temperature of those two precursors at 250, 260, 280, 300, and 320 °C. To obtain UV-vis spectrums, the same amount (0.5 mL) of aliquots was taken 30 minutes after mixing at the corresponding temperatures. Figure 1 shows the UV-vis spectrum for bare ZnSe core synthesized at various reaction conditions. For the ZnSe at 250 °C and 260 °C, only a broad shoulder peaks appeared at the 300 nm wavelength regions; however, the core prepared at 280, 300, and 320 °C showed additional absorption peaks, appearing at 370, 395 (br), and 389 nm. Solution room temperature PL emission spectrum for the ZnSe is also presented in Figure 2. The best PL intensity was obtained from the ZnSe prepared at 300 °C, which shows a very narrow peak at 440 nm with a calculated PL efficiency of 0.8%. The calculated PL efficiencies for the ZnSe samples prepared at other temperature conditions were in the range of 0.1 to 0.5%. These results are comparable for the previously reported ZnSe nanocrystal in the literature.<sup>18</sup>

Selecting the capping material depends on the band gap difference and lattice mismatch rate. One of the best matches, from this point, for the ZnSe must be ZnS, where the band gaps for ZnSe is 2.72 eV and 3.80 eV for ZnS. In addition, the lattice mismatch for the ZnS with the core ZnSe is about 4.6%.<sup>19</sup> The shell layer was also prepared via organometallic zinc precursor with (TMS)<sub>2</sub>S. The reaction temperatures for the shell formation were varied at 125, 135,

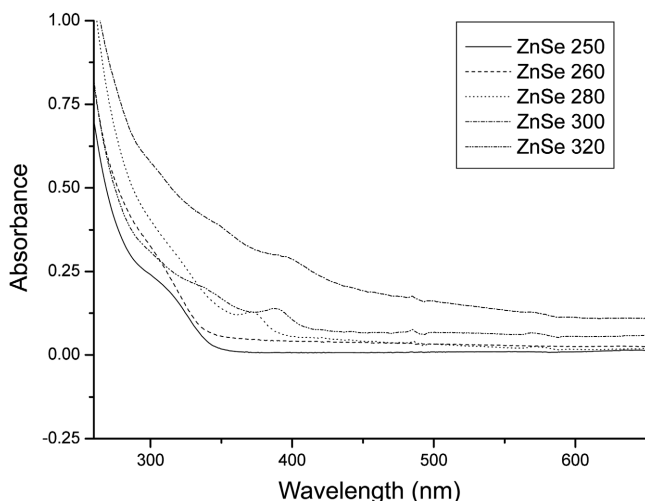


**Figure 1.** UV-Vis spectrum for the core ZnSe synthesized at various temperatures.

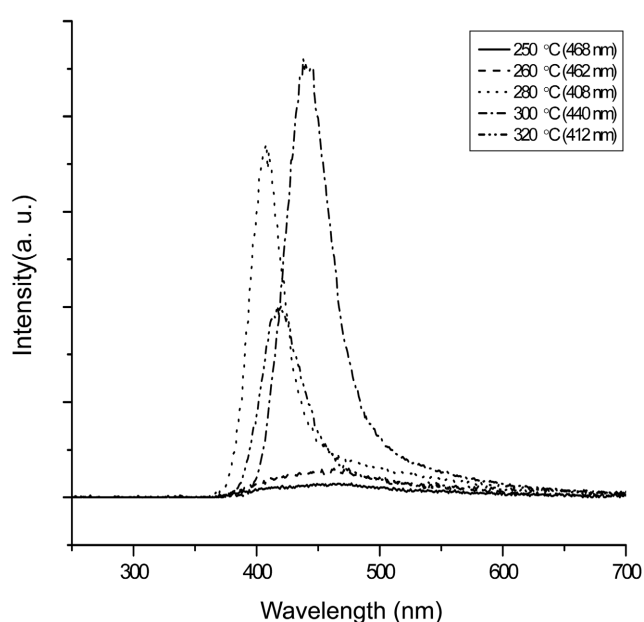


**Figure 2.** Emission spectrum for ZnSe nanocrystals synthesized at various reaction temperatures.

155, 175, and 195 °C respectively. Figure 3 presents the room temperature solution PL emission spectrum for the ZnSe/ZnS core-shell quantum dots dispersed in hexane. Obviously from this figure, the best PL intensity is obtained from the quantum dot that was capped at 135 °C. The best PL intensity is obtained from the ZnSe/ZnS core shell quantum dot that the shell was capped at 135 °C. At this temperature the calculated PL efficiency was 15%, while that for the quantum dots prepared at other shell capping temperatures were in the range of 1 to 8%. In Figure 3, a narrow emission peak appears at 427 nm; however, above this temperature, a higher the capping temperature resulted

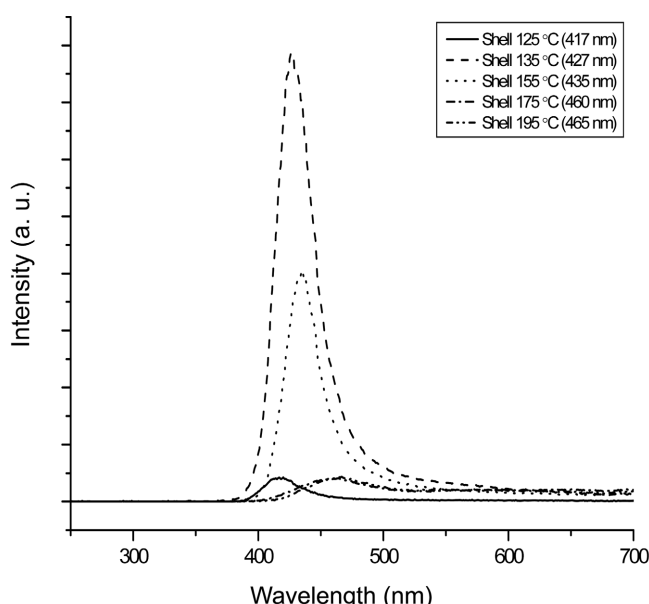


**Figure 3.** Emission spectrum for ZnSe/ZnS quantum dots at various shell capping temperatures.

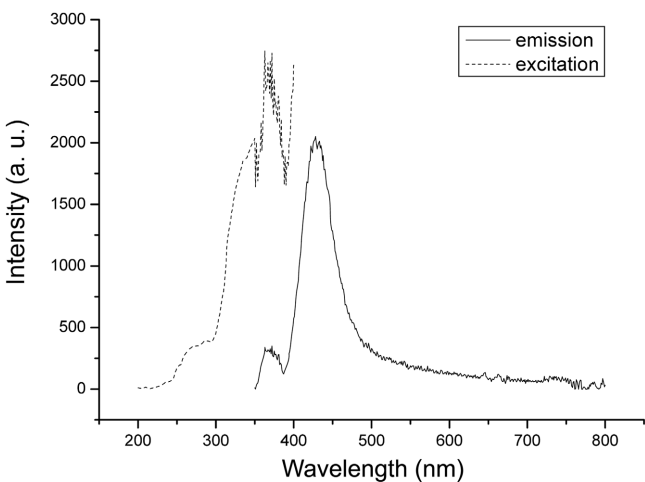


**Figure 4.** Excitation and emission peaks for the ZnSe/ZnS quantum dot.

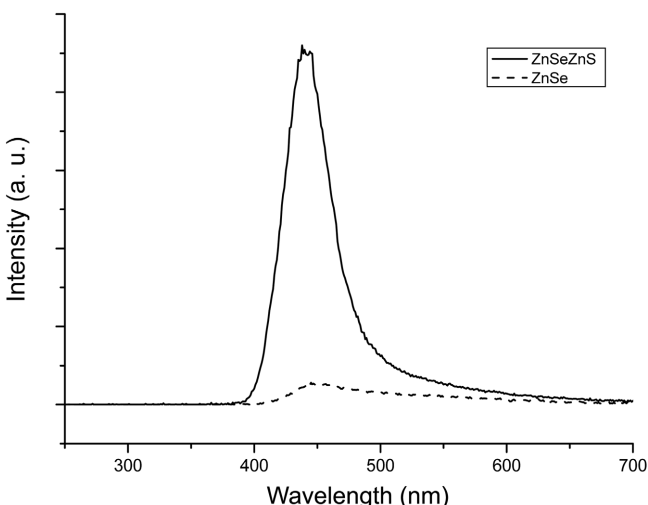


**Figure 5.** Emission spectrum for bare ZnSe and ZnSe/ZnS quantum dot.

in lower PL intensities, and also the emission wavelengths were shifted from 435 to 465 nm. The excitation peaks for the sample capped at this temperature is presented in Figure 4, where the peak appears from 300 nm and the maximum peak is at 367 nm. All the PL emission spectra for the quantum dots were obtained by fixing the excitation wavelength at 367 nm respectively.

Capping the surface of a nanosize material has been shown to cause a remarkable increase in PL intensity.<sup>9,17</sup> The passivation of the core does not change absorption or emission features but greatly increases the quantum yield.<sup>20</sup> We obtained a very similar result, as shown in Figure 5. The obtained best PL efficiency was 15% which increased approximately 20 times more than the bare ZnSe nanocrystal.

The powder XRD spectrum for the ZnSe/ZnS quantum dot is presented in Figure 6. The peak pattern implies that the ZnSe/ZnS quantum dot forms a zinc blende structure in the solid state. In addition, the EDXS spectrum was

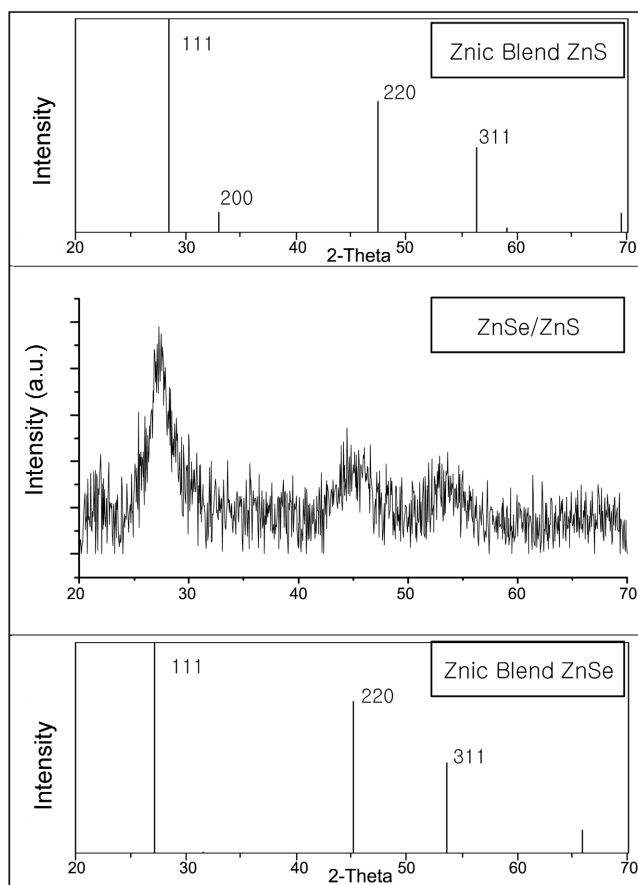


**Figure 6.** Powder XRD patterns for ZnSe/ZnS quantum dot.

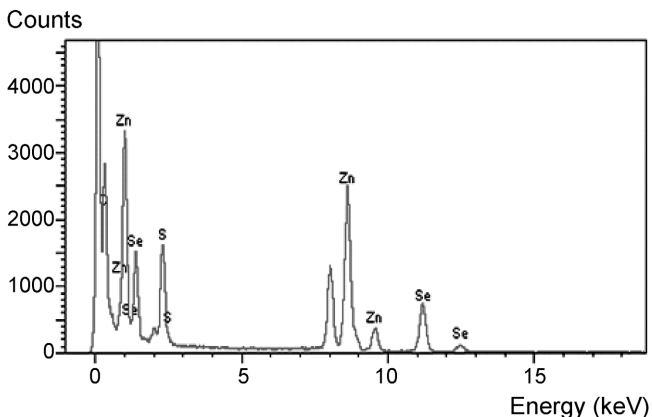


**Figure 7.** EDXS spectrum of the ZnSe/ZnS core-shell quantum dot.

provided in Figure 7, which shows that the elemental compositions of the solid. The spectrum confirms the formation of the ZnSe/ZnS core-shell quantum dot. Both of the XRD and EDXS (TEM) data were obtained from a powder sample of the ZnSe/ZnS quantum dot that the core was formed at 300 °C and the shell capping was performed at 135 °C. The powder was obtained by the addition of 10 mL of absolute ethanol to the ZnSe/ZnS containing solution to yield white precipitation followed by centrifuging and filtering to separate the solid.



**Figure 8.** TEM image of ZnSe/ZnS core/shell quantum dot at  $2 \times 10^3$  fold magnified (scale bar represents 20 nm).

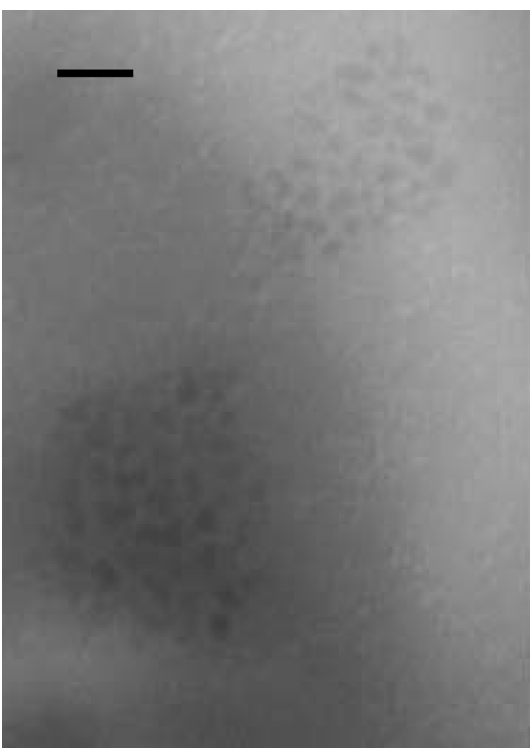


**Figure 8-1.** Regional TEM image of ZnSe/ZnS core/shell quantum dot at  $2 \times 10^3$  fold (scale bar represents 20 nm).

The particle size of the quantum dot was measured *via* a TEM image as presented in Figure 8. According to the picture, the shapes of the particles are homogeneous and the

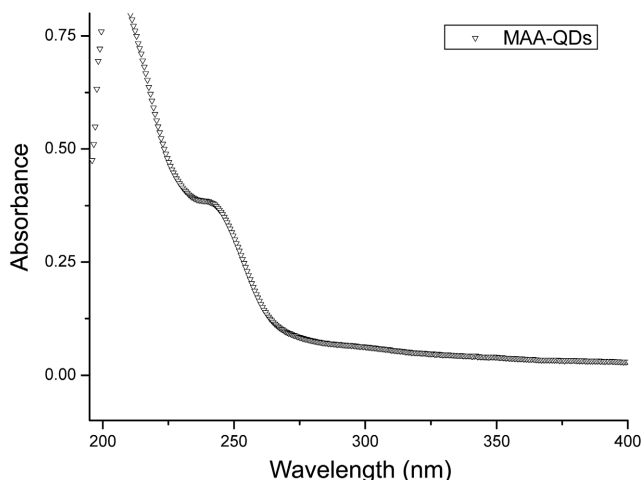


**Figure 9.** UV-vis spectrum for the aqueous colloidal solution of ZnSe/ZnS.

particle sizes are in the range of 5 to 12 nm, which are marginally bigger than the previously reported ZnSe/ZnS nanocomposite (4.6-6 nm).<sup>9</sup> For the bare ZnSe and hydrophobic ZnSe/ZnS quantum dot, they were expected to form spherical or ellipsoidal shapes since they were prepared in a hot coordinating solvent environment. In a dynamic liquid phase, the surface atoms freely and dynamically move to reduce the surface area and unfavorable surface interactions.<sup>9</sup>

Water-soluble semiconductor nanocrystals were developed for fluorescent labeling technologies especially to be applied in biology.<sup>11,18</sup> Unfortunately, most highly luminescent semiconductor nanocrystals are grown in hydrophobic media so that they are hardly compatible with biological systems. There are several reports of solubilized hydrophobic nanocrystals in water.<sup>21-23</sup> For instance, the surface of CdSe/ZnS semiconductor nanocrystal were coated with silica, mercaptoacetic acid, or dihydolipoic acid in buffer solution and they were claimed to be water soluble semiconductor nanocrystals. In the present paper we applied the capping method using deprotonated mercaptoacetic acid (MAA) in a PBS buffer solution for the ZnSe/ZnS quantum dot. Figure 9 shows a UV-vis spectrum of colloidal aqueous solution containing MAA capped ZnSe/ZnS nanocrystal. A broad absorption peak appears at 250 nm. Interestingly the absorption peak was more blue-shifted than the hydrophobic ZnSe/ZnS quantum dot. A similar phenomenon was observed for the water soluble CdS quantum dot capped by bis(2-ethylhexyl) sulfosuccinate (AOT) molecules.<sup>24</sup> According to the authors, that was resulted from the fact that the particles size distribution was relatively narrow in aqueous solution. We think it is also applicable explanation for our case because before we synthesize the water soluble quantum dot by capping with MAA, we performed a size selective precipitation process to isolate solid of hydrophobic ZnSe/ZnS *via* multiple centrifuging and filtering steps.

The room temperature solution PL emission spectrum is

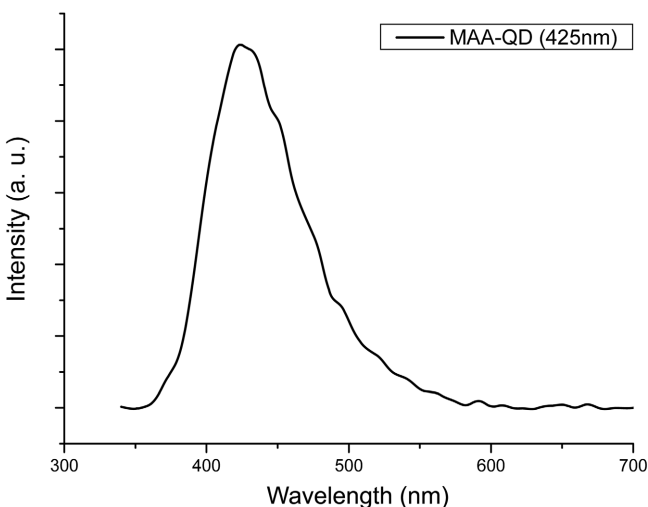


**Figure 10.** Emission spectrum for the aqueous colloidal solution of ZnSe/ZnS.

presented in Figure 10, which shows a broad peak at 425 nm. The calculated PL efficiency for the water soluble quantum dot was about 0.1% which is much lower than the non polar ZnSe/ZnS quantum dot. This is probably resulted from the presence of water molecules and MAA molecules in the same solution which carry lone pair electrons and charges to quench the luminescence of the quantum dot in solution. The similar phenomenon was observed for the previously mentioned water soluble CdS quantum dot capped by AOT molecules.<sup>24</sup>

The large Stoke shift in our excitation and emission spectra for the MAA-capped ZnSe/ZnS quantum dot spectrum is not commonly observed for other semiconductor nanocrystallites. However, a similar feature had been observed for also previously mentioned water soluble CdS nanocrystal. The excitation peak appeared at 400 nm and the emission peak appeared at 540 nm, which showed a 140 nm shift. According to the authors, the phenomenon was due to the recombination of trapped charge carriers as opposed to free carriers. The trapping of the charge carriers occurs at surface defects that lie between the band gap states.<sup>24</sup>

The capping ligand, mercaptoacetate molecule, was also characterized by FT-IR spectroscopy, and the spectrum is shown in Figure 11. To prepare a sample for IR spectroscopy, the aqueous solution containing quantum dot was evaporated under vacuum to yield some sticky pale yellow oil. The free mercaptoacetate molecules were removed by further drying in a vacuum oven for overnight at 60 °C. As a result no recognizable peaks for free MAA molecule were found in the presented IR spectrum. A strong carbonyl peak appeared at  $1575\text{ cm}^{-1}$  which is very similar to that for mercaptoacetic acid coordinated to the surface of silver metal plate in water ( $1560\text{ cm}^{-1}$ ).<sup>25</sup>

Even though we have tried more than five times, we were not able to obtain a well distributed particle image in any of the TEM pictures. This may be due to the strong hydrogen bonding interactions between the capping MAA molecules which make them difficult to separate completely during the

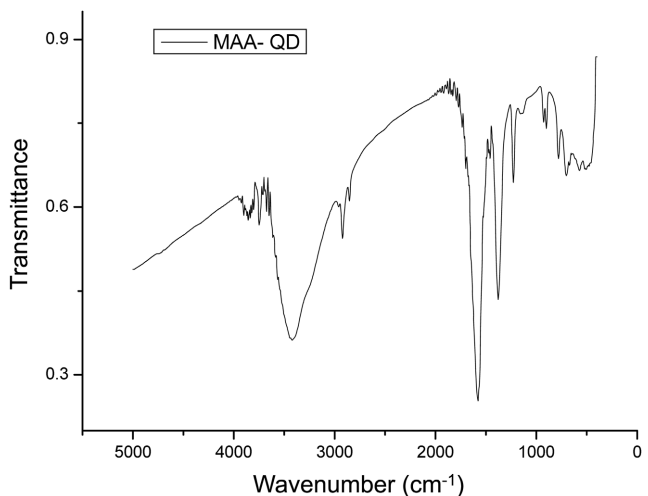


**Figure 11.** FT-IR spectrum of the water soluble ZnSe/ZnS quantum dot.

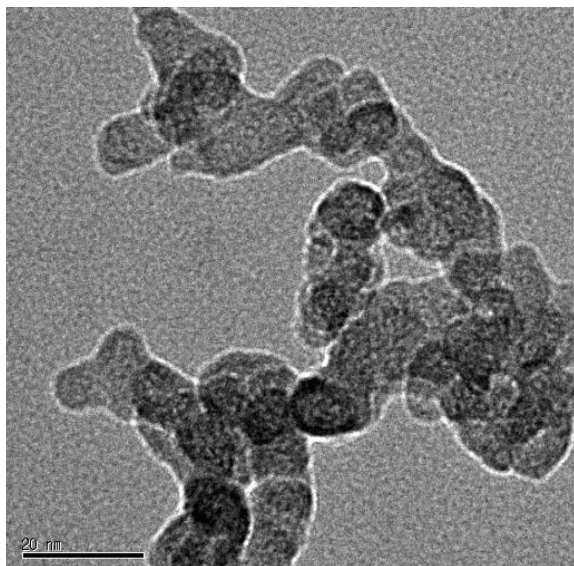


**Figure 12.** TEM image of MAA capped ZnSe/ZnS QD at  $2 \times 10^5$ -fold (the scale bar represents 20 nm).

vacuum drying process. According to the TEM images for the MAA-capped quantum dots, they were in similar spherical and ellipsoidal shapes compared to the bare ZnSe and the hydrophobic ZnSe/ZnS core shell quantum dot particles even though the particle sizes are looked to be little bit bigger than them. However, the bigger particle sizes in the picture do not conclude that the original ZnSe/ZnS particles were growing during replacing the surface with MAA molecules since we did not observe any significant red shift in the absorption peak for the MAA capped ZnSe/ZnS compared with that for the hydrophobic ZnSe/ZnS quantum dot. Therefore, one can say that the surface of the ZnSe/ZnS quantum dot does not really change during the polar MAA molecules replace the originally coordinated TOPO molecules so that they retain the spherical and ellipsoidal shapes in different media.

## Conclusion

In the present study we have synthesized UV-blue luminescent ZnSe/ZnS core shell quantum dots at various reaction conditions. The ZnSe/ZnS quantum dots have been synthesized via a thermal decomposition reaction of organometallic zinc and solvent coordinated Se, (TOP)Se, in a hot HDA/TOP solvent mixture. To optimize the synthetic conditions to yield the best PL intensity, the synthetic conditions for core (ZnSe) and the shell (ZnS) were independently monitored at various temperatures. As a result, we were able to obtain the best PL emission intensity for the ZnSe core at 300 °C, and for the shell capping at 135 °C, in which 5 to 12 nm size of nanoparticles were formed. The best PL efficiencies for the corresponding the ZnSe nanocrystal and the ZnSe/ZnS core-shell quantum dot were 0.8% and 15%, which greatly increased quantum yield up to 20 times more than the bare ZnSe. Furthermore, we have synthesized water-soluble ZnSe/ZnS nanoparticles by capping the ZnSe/ZnS hydrophobic surface with mercapto-acetate (MAA) molecules. For the obtained aqueous colloidal solution, the UV-vis spectrum showed an absorption peak at 250 nm, and the solution PL emission spectrum showed a peak at 425 nm, which is similar to that for hydrophobic quantum dot ZnSe/ZnS. However, the calculated PL efficiency was relatively low (0.1%) due to luminescence quenching by water and charged MAA molecules. The capping ligand was also characterized by FT-IR spectroscopy, with the carbonyl stretching peak in the mercapto-acetate molecule appearing at 1575 cm<sup>-1</sup>. Finally, the particle sizes of the MAA capped ZnSe/ZnS were measured by TEM, showing a range of 12 to 17 nm.

One of the reasons that we synthesized the water-soluble semiconductor nanocrystals is binding them to biomolecules, such as DNA and protein, so that they can be used as a biosensor. In that point of view, even though our water soluble ZnSe/ZnS quantum dot showed a relatively low PL efficiency, it would be sufficiently applicable to a microchip-scale biosensor system. Further bioconjugation study for the water soluble ZnSe/ZnS nanocrystal is progressing in our lab.

**Acknowledgement.** This research was supported by the Faculty Research Fund offered in Dankook University 2004.

## References

- Alivisatos, P. J. *J. Phys. Chem.* **1996**, *100*, 13226.
- Murray, C. B.; Norris, D. J.; Bawendi, M. G. *J. Am. Chem. Soc.* **1993**, *115*, 8706.
- Milliron, D. J.; Alivisatos, A. P.; Pitois, C.; Edder, C.; Frechet, J. M. *J. Adv. Mater.* **2003**, *15*, 58.
- Jaiswal, J. K.; Matoussi, H.; Mauro, J. M.; Simon, S. M. *Nature Biotechnol.* **2002**, *21*, 47.
- Heath, J. R. *Acc. Chem. Res.* **1999**, *32*.
- Hines, M. A.; Guyot-Sionnest, P. *J. Phys. Chem. B* **1998**, *102*, 3655.
- Revaprasadu, N.; Malik, M. A.; O'Brien, P. *J. Mater. Chem.* **1998**, *8*, 1885.
- Chestnoy, N.; Hull, R.; Brus, L. E. *J. Chem. Phys.* **1986**, *85*, 2237.
- Song, K. K.; Lee, S. H. *Curr. Appl. Phys.* **2001**, *1*, 169.
- Matoussi, H.; Mauro, J. M.; Goldman, E. R.; Anderson, G. P.; Sundar, V. C.; Mikulec, F. V.; Bawendi, M. G. *J. Am. Chem. Soc.* **2000**, *122*, 12142.
- Chan, W. C. W.; Nie, S. *Science* **1998**, *281*, 2016.
- Alivisatos, P. *Science* **1996**, *271*, 933.
- Scmidt, M.; Grun, M.; Petillon, S.; Kurtz, E.; Klingshirn, C. *Appl. Phys. Lett.* **2000**, *77*, 85.
- Shavel, A.; Gaponik, N.; Eychmuller, A. *J. Phys. Chem. B* **2004**, *108*, 5905.
- Melhuish, W. H. *J. Phys. Chem.* **1961**, *65*, 229.
- Jun, Y.; Koo, J.; Cheon, J. *Chem. Commun.* **2000**, 1243.
- Ludolph, B.; Malik, M. A.; O'Brien, P.; Revaprasadu, N. *Chem. Commun.* **1998**, 913.
- Reiss, P.; Quemard, G.; Carayon, S.; Bleuse, J.; Chandezon, F.; Pron, A. *Mater. Chem. Phys.* **2004**, *84*, 10.
- Bruchez, S.; Moronne, M.; Gin, P.; Alivisatos, A. P. *Science* **1998**, *281*, 2013.
- Dabbousi, B. O.; Rodriguez-Viejo, J.; Mikulec, F. V.; Heine, J. R.; Matoussi, H.; Ober, R.; Jensen, K. F.; Bawendi, M. G. *J. Phys. Chem. B* **1997**, *101*, 9463.
- Gerion, D.; Pinaud, F.; Williams, S. C.; Parak, W. J.; Zanchet, D.; Weiss, S.; Alivisatos, A. P. *J. Phys. Chem. B* **2001**, *105*, 8861.
- Chen, C. C.; Yet, C. P.; Wang, H. N.; Chao, C. Y. *Langmuir* **1999**, *15*, 6845.
- Mitchell, G. P.; Mirkin, C. A.; Letsinger, R. L. *J. Am. Chem. Soc.* **1999**, *121*, 8122.
- Tata, M.; Banerjee, S.; John, V. T.; Waguestack, Y.; Mcpherson, G. *Coll. Surf. A Phys. Chem. and Eng. Asp.* **1997**, *127*, 39.
- Chung, C. K.; Lee, M. H. *Bull. Korean Chem. Soc.* **2004**, *25*(10), 1461.